Available online at www.sciencedirect.com
ScienceDirect
Trans. Nonferrous Met. Soc. China 26(2016) 2633−2640
Transactions of Nonferrous Metals Society of China
www.tnmsc.cn

Effects of melt overheating degree on undercooling degree and amorphous forming of $Nd_9Fe_{85-x}Ti_4C_2B_x$ (x=10, 12) magnetic alloys

Meng-lin YANG, Jing PAN, Xin-cai LIU, Xiao-yan XIAO, Yu-yong ZHAN

Faculty of Materials Science and Chemical Engineering, Ningbo University, Ningbo 315211, China

Received 1 October 2015; accepted 24 February 2016

Abstract: The effects of melt overheating degree on the undercooling degree and resultant solidification structures of $Nd_9Fe_{85-x}Ti_4C_2B_x$ (x=10, 12) glass-forming alloys were studied by differential thermal analysis combining with solidification structure analysis. The results indicate that the undercooling degree of $Nd_9Fe_{85-x}Ti_4C_2B_x$ (x=10, 12) alloys significantly increases with the rise of melt overheating degree, and two overheating degree thresholds corresponding to the drastic increase of the mean undercooling degree are found for each of the alloys. The existence of two turning points of the mean undercooling degrees can be linked to the structure transitions inside the overheated melts, which result in the evident increase of volume fraction of amorphous phase in the solidified structures.

Key words: magnetic alloy; melt overheating; undercooling degree; structure transition; glass formability

1 Introduction

Recently, bulk $Nd_{7-10}Fe_{bal}B_{10-15}$ nanocomposite permanent magnets which mainly contain $Nd_2Fe_{14}B$, Fe_3B and α-Fe nanocrystallines prepared by copper mold suction casting and subsequent annealing have attracted considerable research interests due to their enhanced coercivity arising from larger volume fraction of hard magnetic phase $Nd_2Fe_{14}B$ of the alloys than that of typical $Fe_3B/Nd_2Fe_{14}B$ type nanocomposites which generally contain 3%−4% Nd and 19%−21% B (mole fraction). Thus, their application prospect in sensors and micro motors is wide. The reported researches were focused on improving the glass-forming ability (GFA) and magnetic properties of the alloys by adding small amount of elements, such as Ti, Nb, Zr, Cr, C, Ga and Co [1−9]. Among these element investigations, the Ti and C co-substitution in $Nd_{7-10}Fe_{bal}B_{10-15}$ alloys leads to a unique advantage of enhancing both the remanence and the coercivity of the alloys, resulting from the effectively refined nanocrystallines caused by the precipitation of TiC at the grain boundary [2,5]. However, the diameters or thicknesses of the bulk $Nd_{7-10}Fe_{bal}B_{10-15}$ magnets reported were ranged in 0.7−1.5 mm (usually just 0.7−1 mm), due to the GFA limited by their low B content as well as the sub-rapidly cooling rate (usually 10^2−10^3 K/s) provided by copper mold suction casting.

It is known that the GFA of an alloy correlates with the ability of its melt to deep undercooling. Previous studies indicated that the melt overheating treatment is an effective method for some glass-forming alloys to significantly improve their undercooling degree and thus their GFA [10−14]. In particular, SHENG et al [10] reported that the volume fraction of the amorphous phase in $Nd_2Fe_{14}B/\alpha$-Fe type $Nd_{9.5}Fe_{81}Zr_3B_{6.5}$ ribbon increased with increasing its melt overheating temperature. However, the relationship between the melt overheating and the resulting undercooling is far from being understood. The experimental results in Refs. [15−20] showed that the dependence of undercooling degree on the melt overheating degree in some metallic melts is nonlinear and discontinuous due to the structure transitions of overheating melts, which is different from the prediction of the theoretical linear relationship between them based on the assumption of the existence of microcavities either on the container or on the surface of impurity particles inside a melt. TONG and SHI [17] demonstrated that the dependence of the degree of undercooling on the level of melt overheating in the Bi

Foundation item: Projects (51174121, 51274125) supported by the National Natural Science Foundation of China; Project (2010R50016-30) supported by Zhejiang Province Science and Technology Innovation Team of Key Projects, China; Project supported by the K. C. Wong Magna Fund of Ningbo University, China
Corresponding author: Jing PAN; Tel: +86-574-87600392; E-mail: panjing@nbu.edu.cn
DOI: 10.1016/S1003-6326(16)64389-3

melt can be either abrupt or continuous, depending on the duration of melt overheating time. MUKHERJEE et al [18] found the overheating temperature thresholds for $Zr_{41.2}Ti_{13.8}Cu_{12.5}Ni_{10}Be_{22.5}$, $Zr_{57}Cu_{15.4}Ni_{12.6}Al_{10}Nb_5$ and $Zr_{52.5}Cu_{17.9}Ni_{14.6}Al_{10}Ti_5$, and that the cooling level in each of the alloy melts would be drastically increased by overheating above their respective threshold temperatures. CHEN et al [19] presented that when the overheating degree of Sb−4.6%Bi alloy was in the range of 150−170 K, the undercooling degree increased dramatically by about 20 K. The research reported by WANG et al [20] showed that the undercooling of $Co_{83}B_{17}$ alloy was greatly affected by the overheating temperature and a turning point of mean undercooling existed when the overheating temperature exceeded a threshold value. However, up to now, only a few alloy systems that exhibit distinctive overheating effect are found, and there is still no reported research involving the melt overheating treatment of $Nd_{7-10}Fe_{bal}B_{10-15}$ based alloys which may be a possible way to increase their undercooling degree and thus enhance their GFA with other factors remaining unchanged. In this work, by using differential thermal analysis (DTA) we investigated the dependence of the undercooling degree (ΔT^-) on the overheating degree (ΔT^+) in the $Nd_9Fe_{85-x}Ti_4C_2B_x$ (x=10, 12) melts for their particularities of containing lower B content comparing with other $Nd_{7-10}Fe_{bal}B_{10-15}$ based alloys, and two ΔT^+ thresholds of the melts corresponding to the drastic increase of the mean ΔT^- for the alloys were found, which indeed resulted in the significant increase of the volume fraction of amorphous phase in the solidified alloys, which was confirmed by the variation of the crystallization enthalpies in the DSC curves of the alloy samples.

2 Experimental

Alloy ingots with nominal composition of $Nd_9Fe_{85-x}Ti_4C_2B_x$ (x=10, 12) were prepared by arc melting mixtures of 99.99% Nd, 99.5% Fe, Ti, C and Fe−20%B (mass fraction) intermediate alloy in a high purity argon atmosphere. The button-shaped ingots were re-melted six times to ensure good homogeneity.

DTA is a powerful tool for investigating the relationship between the ΔT^+ and the ΔT^- because it is able to provide not only the most accurate temperature control, but also an accurate control of the rates of melt cooling and heating. However, a major difficulty existing in the DTA test for Nd−Fe−B alloys is that the alloys are easy to be oxidized. Hence, a set of vacuum system was established firstly in a NETZSCH DSC 404F1 difference scanning calorimeter. DTA curves of the alloys were measured by this difference scanning calorimeter which was pre-evacuated to 1×10^{-2} Pa and refilled with a continuous flow of highly purified argon to prevent the alloys from oxidation, and a faster heating/cooling rate, 40 K/min, was employed in DTA test to prevent the high temperature melts from evaporation. Each of the alloys was heated up to a series of overheating temperature (T^+) (1503, 1523, 1543, 1563, 1583, 1603, 1623 and 1643 K) and then cooled down. The liquidus temperature (T_L) was determined by the end temperature (extrapolated finish) of the final endothermic peak on the heating curve, the solidus temperature (T_S) was determined by the point of the beginning of the differential record deviation from the baseline (extrapolated onset) on the heating curve, and the initial nucleation temperature (T_N) was determined by the initial temperature (extrapolated onset) of the first exothermic peak on the cooling curve by using NETZSCH-Proteus software that the instrument came with.

The phase structures of the samples were investigated using D8 Focus X-ray diffraction (XRD) with Cu K_α radiation, and the microscopic morphologies of the samples were observed using Quanta250 FEG scanning electron microscope (SEM). The micro area composition was measured by energy dispersive spectrometer (EDS) attached in the SEM. The crystallizing temperatures and the crystallization enthalpies of the samples were determined using a NETZSCH DSC 404F1.

3 Results and discussion

3.1 Determination of characteristic temperatures by DTA

Figures 1 and 2 show the DTA heating curves of the $Nd_9Fe_{85-x}Ti_4C_2B_x$ (x=10, 12) alloys which were respectively heated up to a series of T^+ (1503, 1523, 1543, 1563, 1583, 1603, 1623 and 1643 K). The measured liquidus temperature $T_{L,m}$ and solidus temperature $T_{S,m}$ on each heating curve of the alloy with eight different T^+ are slightly different due to experimental error. The $T_{L,m}$ and $T_{S,m}$ as well as their arithmetic average T_L and T_S are listed in Table 1.

Figures 3 and 4 show the DTA cooling curves of the $Nd_9Fe_{85-x}Ti_4C_2B_x$ (x=10, 12) alloys which were respectively heated up to a series of T^+ (1503, 1523, 1543, 1563, 1583, 1603, 1623 and 1643 K) and then cooled down. The measured initial nucleation temperatures T_N on each cooling curves of the alloys are listed in Table 1. It can be seen that with the increase of the T^+ of melts from 1503 to 1643 K, the T_N of the alloy melts gradually decreases.

The values of melt overheating degree ΔT^+ ($\Delta T^+=T^+-T_L$) and its undercooling degree ΔT^- ($\Delta T^-=T_L-T_N$) corresponding to the varied T^+ are also listed in Table 1.

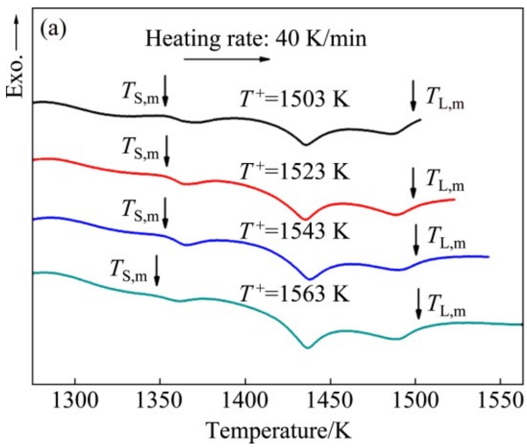

Fig. 1 DTA heating curves for $Nd_9Fe_{75}Ti_4C_2B_{10}$ alloy with various overheating temperatures

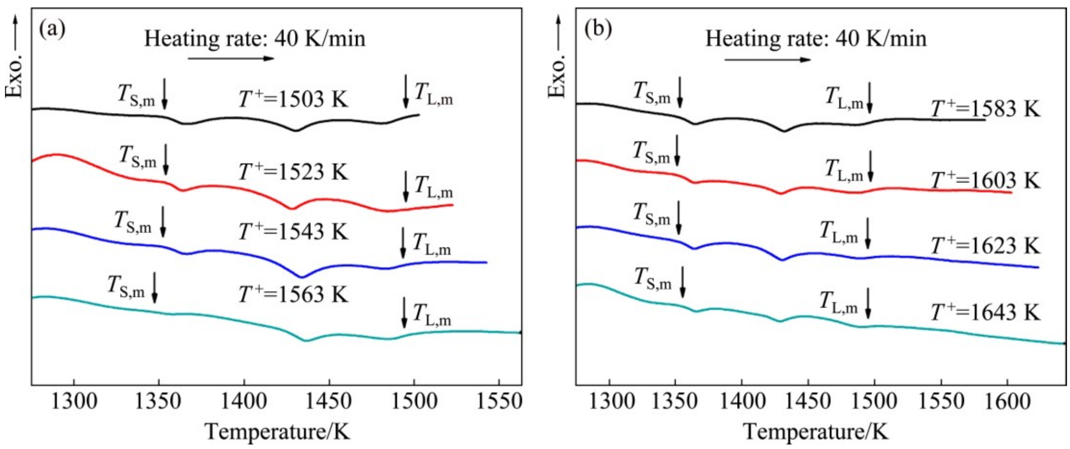

Fig. 2 DTA heating curves for $Nd_9Fe_{73}Ti_4C_2B_{12}$ alloy with various overheating temperatures

Table 1 Solidus temperature, liquidus temperature, nucleation temperature, melt overheating degree and nucleation undercooling degree of $Nd_9Fe_{85-x}Ti_4C_2B_x$ (x=10, 12) alloys with various melt overheating temperatures determined from DTA curves

x/%	T^+/K	$T_{S,m}$/K	T_S/K	$T_{L,m}$/K	T_L/K	T_N/K	ΔT^+/K	ΔT^-/K
10	1503	1353.4	1352.1	1498.5	1501.6	1375.6	1.4	126.0
	1523	1353.8		1498.3		1373.0	21.4	128.6
	1543	1353.7		1499.9		1349.2	41.4	152.4
	1563	1347.5		1502.4		1350.9	61.4	150.7
	1583	1347.1		1504.7		1349.8	81.4	151.8
	1603	1352.1		1503.5		1337.5	101.4	164.1
	1623	1354.6		1503.9		1334.6	121.4	167.0
	1643	1354.2		1501.9		1335.3	141.4	166.3
12	1503	1354.3	1353.3	1495.9	1495.4	1377.0	7.6	118.4
	1523	1355.7		1496.0		1376.0	27.6	119.4
	1543	1354.1		1495.2		1332.5	47.6	162.9
	1563	1347.6		1495.7		1328.4	67.6	167.0
	1583	1353.5		1495.5		1327.7	87.6	167.7
	1603	1352.5		1496.2		1315.7	107.6	179.7
	1623	1353.4		1494.6		1317.4	127.6	178.0
	1643	1355.5		1493.8		1318.3	147.6	177.1

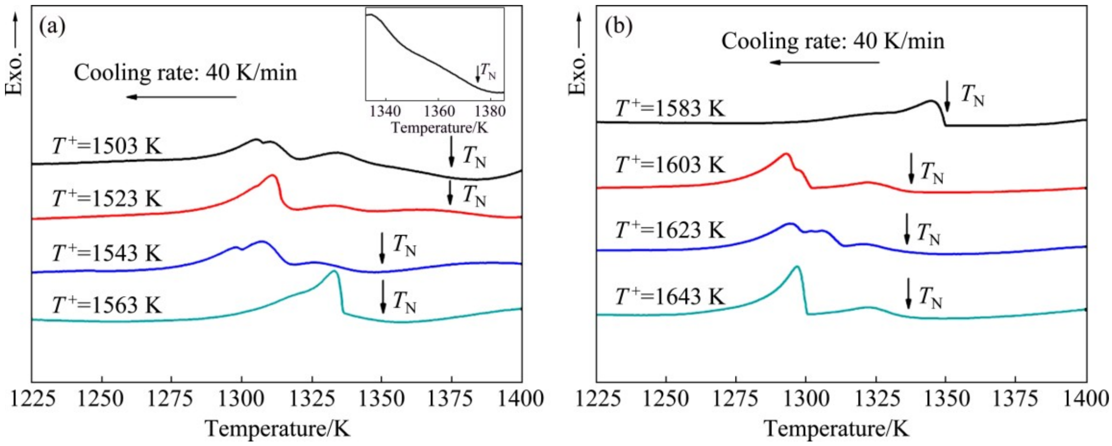

Fig. 3 DTA cooling curves for $Nd_9Fe_{75}Ti_4C_2B_{10}$ alloy with various overheating temperatures (The insert is a partial enlarged drawing of the cooling curve with overheating temperature T^+ of 1503 K)

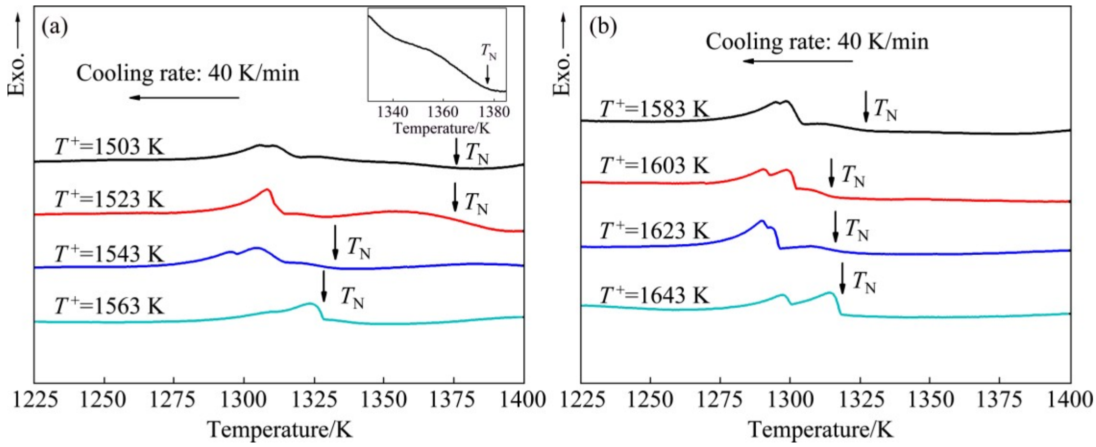

Fig. 4 DTA cooling curves for $Nd_9Fe_{73}Ti_4C_2B_{12}$ alloy with various overheating temperatures (The insert is a partial enlarged drawing of the cooling curve with overheating temperature T^+ of 1503 K)

The results indicate that the ΔT^- values of $Nd_9Fe_{85-x}Ti_4C_2B_x$ (x=10, 12) alloys have reached 126.0 and 118.4 K alloys with x=10 and 12 respectively when their T^+ just reaches 1503 K which are very close to their liquidus temperatures. The XRD patterns of the precursor ingots and the samples after DTA with their T^+ of 1503 K are shown in Fig. 5. Some sharp crystalline diffraction peaks corresponding to $Nd_2Fe_{14}B$, Fe_3B, α-Fe, $Nd_{1.1}Fe_4B_4$ and TiC respectively can be seen in all the patterns, and the average grain sizes of all the crystalline phases, estimated from each of XRD patterns based on the Scherrer's formula, are 56 and 54 nm when x=10 and 12 respectively for the alloys before DTA, and are 57 and 55 nm when x=10 and 12 respectively for the alloys after DTA, indicating that the solidification structures of the samples before and after DTA are all mainly composed of non-equilibrium nanocrystallines. Therefore, the studied $Nd_9Fe_{85-x}Ti_4C_2B_x$ (x=10, 12) alloys exhibit a highly undercooling tendency and stronger nanocrystalline forming ability, implying that the alloys may have the strong dependence of the ΔT^- of the melts on their ΔT^+ like other amorphous alloys reported in Refs. [11,14].

3.2 Dependence of undercooling degree on overheating degree

Figure 6 shows the measured results of dependence of the ΔT^- on ΔT^+ in $Nd_9Fe_{85-x}Ti_4C_2B_x$ (x=10, 12) melts. It is obvious that with raising the ΔT^+ of the melts, the resultant ΔT^- increases significantly by about 40 and 60 K, respectively when x=10 and 12. It is worthy to note that there exist two ΔT^+ thresholds that respectively correspond to the two mean ΔT^- turning points during the overheating process of the melts. For the alloy with x=10, the mean ΔT^- is about 127 K when the ΔT^+ is below about 30 K, while the mean ΔT^- drastically increases to about 151 K when the ΔT^+ surpasses its first threshold value of 41.4 K; and then the mean ΔT^- drastically increases again to about 166 K when the ΔT^+ surpasses its second threshold value of 101.4 K. For the alloy with x=12, the mean ΔT^- is about 119 K when the ΔT^+ is below about 30 K, while the mean ΔT^- drastically

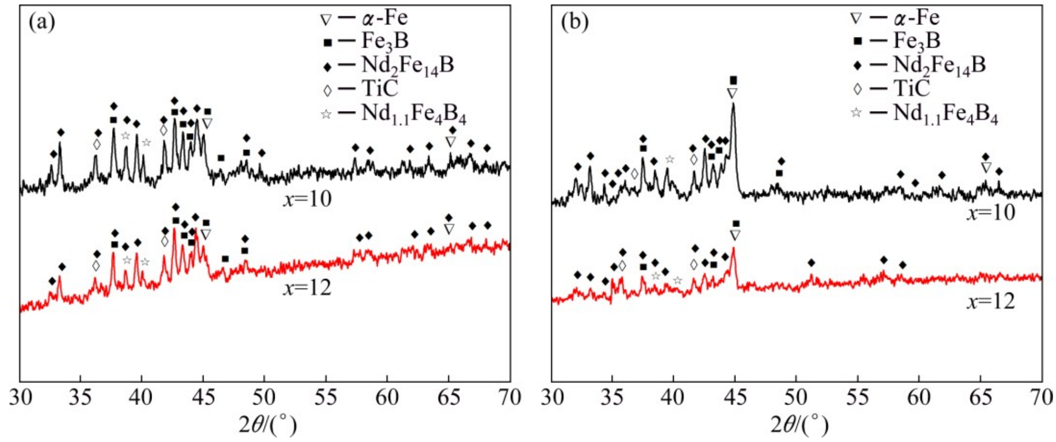

Fig. 5 XRD patterns for $Nd_9Fe_{85-x}Ti_4C_2B_x$(x=10, 12) alloys before (a) and after (b) DTA with their overheating temperature T^+ of 1503 K

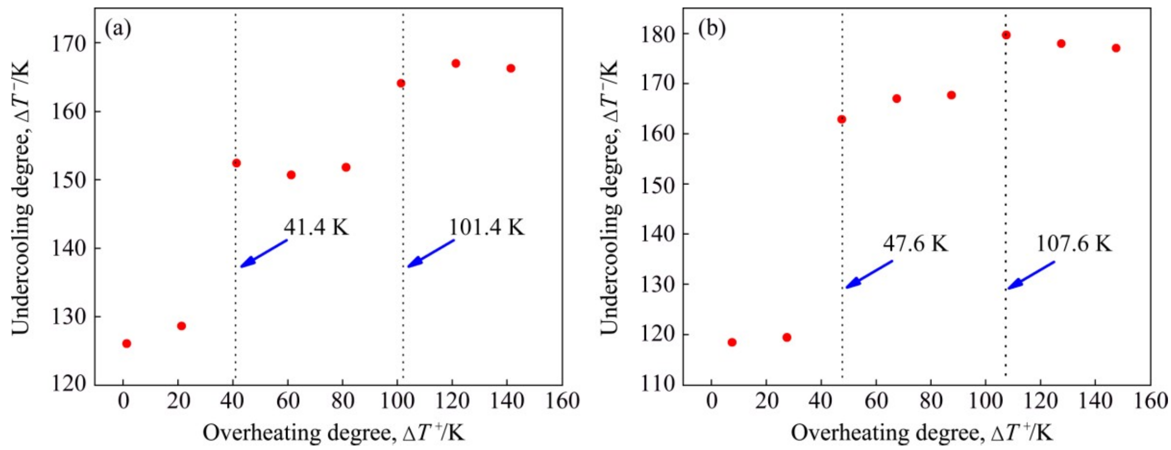

Fig. 6 Dependence of undercooling degree on melt overheating degree for $Nd_9Fe_{85-x}Ti_4C_2B_x$ (x=10, 12) alloys: (a) x=10; (b) x=12

increases to about 165 K when the ΔT^+ surpasses its first threshold value of 47.6 K; and then the mean ΔT^- drastically increases again to about 178 K when the ΔT^+ surpasses its second threshold value of 107.6 K. It can be seen that the ΔT^+ of the $Nd_9Fe_{85-x}Ti_4C_2B_x$ (x=10, 12) melts has strong and distinct impact on their undercooling behavior, and the relationships between the ΔT^- and ΔT^+ in these two melts are so alike.

As reported in Refs. [14,21−23], the atomic bonds in solid crystals are only partially broken during melting, and some short-range order atomic clusters corresponding to crystal structures can exist and remain in overheated melt within a wide range of temperatures above the liquidus temperature. These atomic clusters can act as the intrinsic growth nuclei during the melt cooling; however, they can be minified, reduced or even vanished by elevating the melt overheating temperature, leading to the variation of undercooling. For $Nd_9Fe_{85-x}Ti_4C_2B_x$ (x=10, 12) alloys, as we can see from the XRD results in Fig. 5(a), $Nd_2Fe_{14}B$, Fe_3B, α-Fe, $Nd_{1.1}Fe_4B_4$ and TiC nanocrystalines exist in the precursor ingots. Therefore, at least five kinds of atomic clusters with various compositions exist in the overheated melts, whereas each kind of atomic clusters starts to dissolve at specific overheating temperatures. In particular, among crystals in the precursor ingots refractory compound TiC can start to melt by the way of self-diffusion at temperatures of 30−50 °C above liquidus [23,24]. Consequently, its corresponding atomic clusters in the melts will begin to dissolve at higher overheating temperature than those of other crystals in the melts. Specifically, it can be conjectured that when the ΔT^+ of a melt reaches higher than 40 K (see Fig. 6), some kinds of clusters can be dissolved in a large amount, leading to the first ΔT^- turning point; and then when the ΔT^+ of this melt reaches higher than 100 K, the rest of clusters that might mainly be composed of corresponding atomic clusters of TiC can be dissolved in a large amount, leading to the second ΔT^- turning point. These results demonstrate that in an overheated melt consisting of three components or more, structure transition can occur more than once, which is different from Bi melt and Co−B melt in which only once structure transition was found [17,20].

3.3 Melt structure transition and glass forming ability

To get an evidence of the structure variations in the overheating melts of $Nd_9Fe_{85-x}Ti_4C_2B_x$ (x=10, 12) alloys, the solidified structures of the samples after DTA with T^+ reaching 1523, 1543 and 1643 K, respectively were analyzed, and the typical SEM images (backscattered mode) of samples are shown in Figs. 7 and 8. It can be seen in these micrographs that many dark gray dendrite regions are embedded in the light gray featureless matrix. EDX (attached to SEM) analyses display that the light gray featureless matrix (Spectrum 1) contains 12.15% Nd and 64.86% Fe (mole fraction) when x=10 and 8.66% Nd and 70.66% Fe (mole fraction) when x=12, which are very close to the nominal composition of the precursor ingots; and the dark gray dendrite regions (Spectrum 2) contain 0.41% Nd and 77.52% Fe when x=10, and no Nd and 81.28% Fe when x=12, which are similar to the composition of mixture of $Nd_2Fe_{14}B$, Fe_3B and α-Fe shown in the XRD patterns of Fig. 5. According to these results combining with the reported SEM images (backscattered mode) of partially amorphous structure in Refs. [25,26], it is suggested that the light gray featureless matrix in Figs. 7 and 8 is almost an amorphous structure, and the dark gray dendrite region is a nanocrystalline group mainly consisting of $Nd_2Fe_{14}B$, Fe_3B and α-Fe. Besides, the black acicular regions (Spectrum 3) in Figs. 7 and 8 contain 49.33% Ti and 48.72% C when x=10 and 48.73% Ti and 50.77% C when x=12, which are very close to the composition of TiC shown in the XRD patterns of Fig. 5, suggesting that the black acicular region is the needle-like TiC

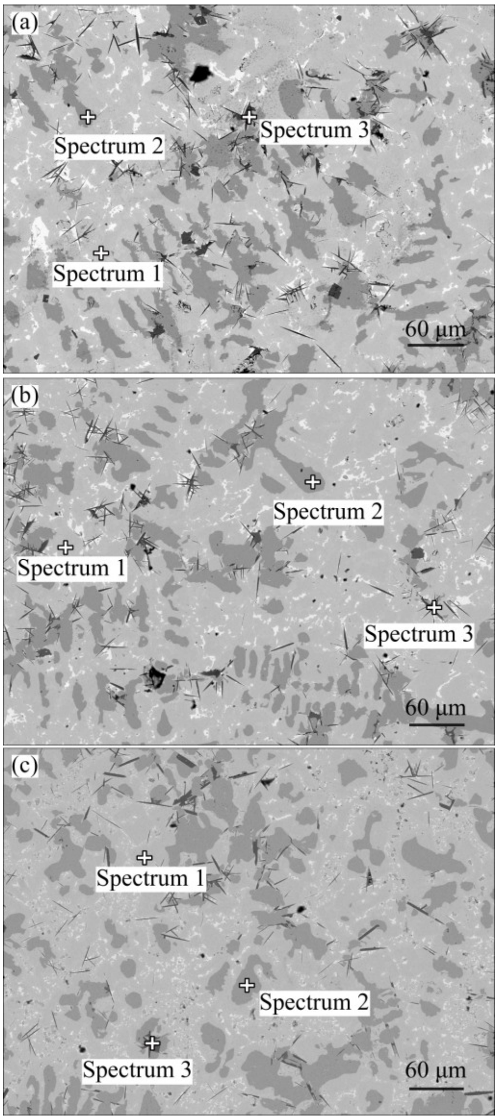

Fig. 7 SEM (backscattered mode) images of solidified $Nd_9Fe_{75}Ti_4C_2B_{10}$ alloy after DTA at different overheating temperatures: (a) T^+=1523 K (ΔT^+=21.4 K, ΔT^-=128.6 K); (b) T^+=1543 K (ΔT^+=41.4 K, ΔT^-=152.4 K); (c) T^+=1643 K (ΔT^+=141.4 K, ΔT^-=166.3 K)

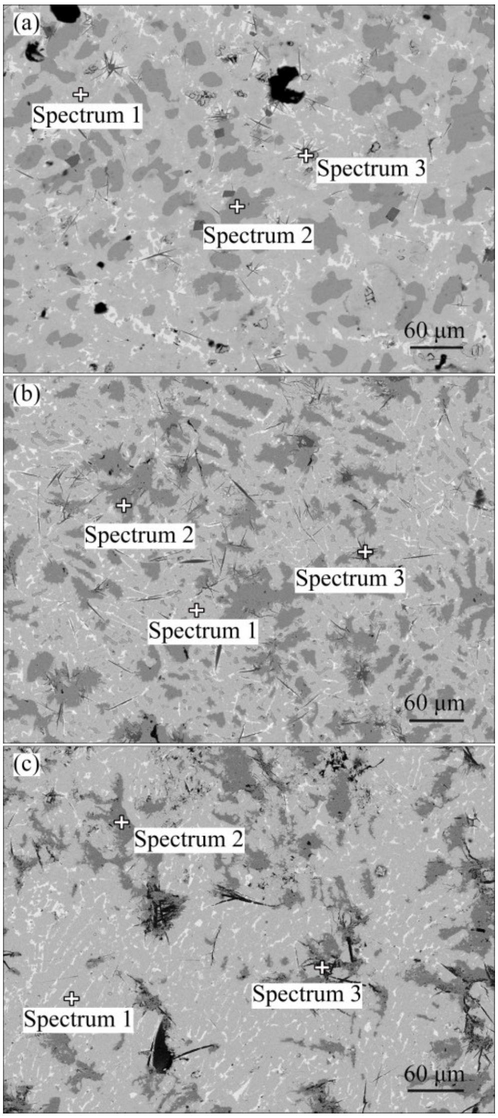

Fig. 8 SEM (backscattered mode) images of solidified $Nd_9Fe_{73}Ti_4C_2B_{12}$ alloy after DTA with different overheating temperatures: (a) T^+=1523 K (ΔT^+=27.6 K, ΔT^-=119.4 K); (b) T^+=1543 K (ΔT^+=47.6 K, ΔT^-=162.9 K); (c) T^+=1643 K (ΔT^+=147.6 K, ΔT^-=177.1 K)

precipitated from the overheated melt when it begins to cool according to Refs. [24]. It can be seen obviously from Figs. 7 and 8 that with the increase of overheating temperature, the volume fraction of the light gray amorphous matrix increases remarkably, whereas the volume fraction of dark gray nanocrystalline group decreases evidently and its dendrite morphology characteristic inherited from the alloy melts of the precursor ingots gradually disappears, indicating that the alloy melts become more and more homogeneous and the nucleation barrier becomes higher and higher with the raise of overheating temperature.

Furthermore, the thermal analysis of the $Nd_9Fe_{73}Ti_4C_2B_{12}$ alloy after DTA with T^+ reaching 1523, 1543 and 1643 K, respectively, was carried out at heating rate of 20 K/min and the DSC curves are shown in Fig. 9. Similar to other $Nd_{7-10}Fe_{bal}B_{10-15}$ based alloys [27], all of T_g on the DSC curves cannot be observed clearly. However, the first crystallization temperatures T_x on the DSC curves, 935.6, 936.3 and 946.0 K for T^+=1523, 1543 and 1643 K, respectively, can be determined accurately. Thus, the corresponding reduced crystallization temperatures T_{rx} (T_x/T_L) of 0.6256, 0.6261 and 0.6326 (T_L=1495.4 K from Table 1) respectively can be obtained, implying that the GFA of the alloy increases with the increase of the T^+ according to Ref. [28]. Moreover, the total crystallization enthalpies in each curve in Fig. 9 calculated by NETZSCH-Proteus software, which reflect the amount of amorphous phase in the alloy, are 14.13, 16.79 and 63.76 J/g for T^+=1523, 1543 and 1643 K, respectively, fully verifying that the volume fraction of amorphous phase in the alloy significantly increases with the raise of melt overheating temperature, which is consistent with the SEM results. And it is noteworthy that the volume fraction of amorphous phase in the alloy drastically increases when the ΔT^+ of the melt surpasses its second threshold value of 107 K. The above results confirm the

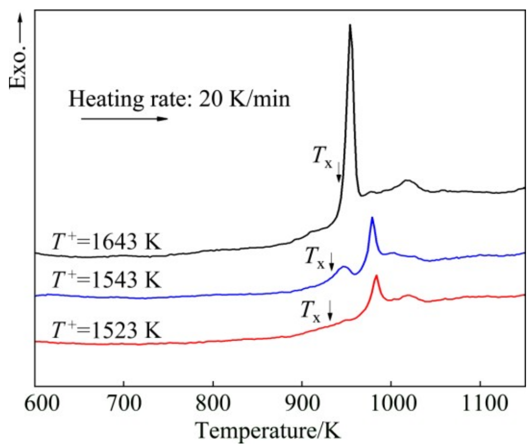

Fig. 9 DSC curves of solidified $Nd_9Fe_{73}Ti_4C_2B_{12}$ alloy after DTA at different overheating temperatures

structure transitions in the overheating melts, and exhibit the enhancement of the GFA of the alloy arising from the melt overheating.

4 Conclusions

1) The undercooling degree values (ΔT^-) of $Nd_9Fe_{85-x}Ti_4C_2B_x$ (x=10, 12) alloy melts were found to be significantly increased by about 40 and 60 K respectively when x=10 and 12 with the raise of their melts overheating degree ΔT^+, and the dependence of the ΔT^- on ΔT^+ in the melts was abrupt. The mean ΔT^- in melts was found to drastically increase respectively when the melt ΔT^+ surpassed the first threshold value of 41.4 K and then the second threshold value of 101.4 K for the melt with x=10; and the first threshold value of 47.6 K and then the second threshold value of 107.6 K for the melt with x=12. The existence of the two turning points of the mean ΔT^- in each of the melts can be linked to the two structure transitions inside the melts caused by successively dissolving at least five kinds of atomic clusters corresponding to the solid crystals in precursor ingots at different overheating temperatures.

2) By raising the melt overheating temperature, the volume fraction of the amorphous phase in the solidified structures of the samples after DTA increased remarkably, whereas the volume fraction of nanocrystalline group decreased evidently and its dendrite morphology characteristic inherited from the overheated melts gradually disappeared, which confirmed the structure variations of the overheating melts and exhibited the enhancement of the GFA arising from the melt overheating.

References

[1] CHANG H W, CHENG Y T, CHANG C W, HSIEH C C, GUO Z H, CHANG W C, SUN A C. Improvement of size and magnetic properties of $Nd_{9.5}Fe_{72.5}Ti_3B_{15}$ bulk magnets by Zr or Nb substitution for Ti [J]. Journal of Applied Physics, 2009, 105: 07A742.

[2] CHANG H W, GAN J Y, HSIEH C C, ZHAO X G, CHANG W C. Effects of C and Cr contents on the magnetic properties and microstructure of directly quenched NdFeTiZrCrBC bulk magnets [J]. Journal of Applied Physics, 2010, 107: 09A740.

[3] CHANG H W, SHIH M F, CHANG C W, HSIEH C C, FANG Y K, CHANG W C, SUN A C. Magnetic properties and microstructure of directly quenched $Nd_{9.5}Fe_{75.5-x}M_xB_{15}$ (M=Mo, Nb, Ta, Ti, V, and Zr; x=0−4) bulk magnets [J]. Journal of Applied Physics, 2008, 103: 07E105.

[4] CHANG H W, SHIH M F, HSIEH C C, CHANG W C. Development of bulk $Nd_{9.5}Fe_{75.5-x}M_xB_{15}$ (M=Mo, Nb, Ta, Ti, and Zr; x=0−4) magnets by direct casting method [J]. Journal of Alloys and Compounds, 2009, 484: 143−146.

[5] CHANG H W, HSIEH C C, GAN J Y, CHENG Y T, SHIN M F, CHANG W C. Alloying effect on the magnetic properties of *R*FeB-type bulk magnets [J]. Journal of Physics D: Applied Physics, 2011, 44: 064002.

[6] WANG C, CHEN J J, LI Y, LUO C L, CHEN W Z. Magnetic

properties, microstructure and corrosion behavior of $Nd_{10}Y_1Fe_{85-x}Nb_{3.5}Ti_{0.5}B_x$ (x=14−22) and $Nd_{10}Y_1Fe_{69}Nb_{3.5}M_{0.5}B_{16}$ (M=Ti, Zr, Cr, Mo) bulk nanocrystalline magnets [J]. Journal of Alloys and Compounds, 2013, 555: 16−21.
[7] LIU Z, HSIEH C C, CHEN R J, LIN W C, CHANG H W, CHANG W C, YAN A R. Magnetic properties, phase and microstructure of direct cast $Nd_{9.5}Fe_{bal}Co_{10}MB_{15}$ rod magnets [J]. Journal of Magnetism and Magnetic Materials, 2013, 326: 108−111.
[8] CHANG H W, SHIN M F, HSIEH C C, CHANG W C, SHEN C Y. Magnetic property enhancement of directly quenched Nd−Fe−B bulk magnets with Ti substitution [J]. Journal of Alloys and Compounds, 2010, 489: 499−503.
[9] JIANG X L, JIANG Y X, PAN J, LIU X C. Microstructures evolution and magnetic properties of copper mold suction casting $Nd_9Fe_{83-x}Ti_4C_4B_x$ (x=10−15) alloys [J]. Journal of the Chinese Society of Rare Earths, 2014, 32(3): 316−321. (in Chinese)
[10] SHENG H C, ZENG X R, QIAN H X, FU D J. Effect of melt treatment on the microstructure and magnetic properties of $Nd_2Fe_{14}B/\alpha$-Fe nanocomposites [J]. Journal of Non-Crystalline Solids, 2010, 356: 19−23.
[11] KOU S Z, LI L, ZHENG B C, ZHAO Y C, XUE S W. Effect of TRT process on the glass forming ability of $Cu_{45}Zr_{42}Al_8Ag_5$ amorphous and DSC study on bulk amorphous alloys [J]. China Foundry Machinery & Technology, 2009, 5: 30−33. (in Chinese)
[12] DENG Y B, WANG X L, GENG H R, WANG Z M, ZHANG L. Effects of melt over-heating treatment on glass forming ability (GFA) of Al-based alloys [J]. Special Casting & Nonferrous Alloys, 2009, 29(8): 756−760. (in Chinese)
[13] LI L, LIU L J, CUI X, WANG Z Z, YANG D D, LV X, ZU F Q. Effect of liquid structure on the crystallization and GFA of $Cu_{40}Zr_{45}Al_7Ag_8$ BMGs [J]. Special Casting & Nonferrous Alloys, 2011, 31(6): 568−571. (in Chinese)
[14] MANOV V, POPEL P, BROOK-LEVINSON E, MOLOKANOV V, CALVO-DAHLBORG M, DAHLBORG U, SIDOROV V, SON L, TARAKANOV Y. Influence of the treatment of melt on the properties of amorphous materials: Ribbons, bulks and glass coated microwires [J]. Materials Science and Engineering A, 2001, 304−306: 54−60.
[15] GUO F X, WANG W, YANG H L, QIN J Y, TIAN X L. Abnormal resistivity and viscosity behavior in Sb-rich Pb−Sb melts [J]. Transactions of Nonferrous Metals Society of China, 2012, 22: 3113−3119.
[16] LIU R S, LIANG Y C, LIU H R, ZHENG N C, MO Y F, HOU Z Y, ZHOU L L, PENG P. Simulation study on non-linear effects of initial melt temperatures on microstructures during solidification process of liquid Mg_7Zn_3 alloy [J]. Transactions of Nonferrous Metals Society of China, 2013, 23: 1052−1060.
[17] TONG H Y, SHI F G. Dependence of supercooling of a liquid on its overheating [J]. Journal of Chemical Physics, 1997, 107(19): 7964−7966.
[18] MUKHERJEE S, ZHOU Z, SCHROERS J, JOHNSON W L, RHIM W K. Overheating threshold and its effect on time− temperature-transformation diagrams of zirconium based bulk metallic glasses [J]. Applied Physics Letters, 2004, 84(24): 5010−5012.
[19] CHEN G, YAN Y B, CUI P, YU J W, LI J S, FU H Z. Effect of melt superheating on solidified structure of a Sb−Bi alloy [J]. Materials Science & Technology, 2001, 9(2): 113−116. (in Chinese)
[20] WANG J, HE Y X, LI J S, HU R, KOU H C, BEAUGNON E. Overheating dependent undercooling in a hypoeutectic Co−B alloy [J]. Materials Chemistry and Physics, 2014, 149−150: 17−20.
[21] LIU X J, HUI X D, CHEN G L. Thermodynamic calculation and experimental investigation of glass formation in Zr−Ni−Ti alloy system [J]. Intermetallics, 2008, 16(2): 262−266.
[22] DAHLBORG U, CALVO-DAHLBORG M, POPEL P S, SIDOROV V E. Structure and properties of some glass-forming liquid alloys [J]. The European Physical Journal B, 2000, 14: 639−648.
[23] GUI Z L. Development of high temperature treatment process of Ni-base superalloy melts [J]. Aero Manufacture Engineering, 1995, 4: 12−14. (in Chinese)
[24] FILIP O, HERMANN R, SCHULTZ L. Growth kinetics and precipitation phenomena in undercooled Nd−Fe−B melts with Ti and C additions [J]. Journal of Magnetism and Magnetic Materials, 2001, 234: 247−254
[25] LU Z P, LIU C T, PORTER W D. Role of yttrium in glass formation of Fe-based bulk metallic glasses [J]. Applied Physics Letters, 2003, 83(13): 2581−2583.
[26] ZHANG J, LIM K Y, FENG Y P, LI Y. Fe−Nd−B-based hard magnets from bulk amorphous precursor [J]. Scripta Materialia, 2007, 56: 943−946.
[27] LIU Z, LIN W C, SHIH C W, HSIEH C C, CHANG H W, CHANG W C, YAN A R. Effect of Co addition on the microstructure and magnetic properties of $Nd_{9.5}Fe_{bal}Co_xNb_{2.5}Zr_{0.5}B_{15}$($x$=0,10,20) bulk magnets [J]. Journal of Alloys and Compounds, 2012, 538: 28−33.
[28] INOUE A, ZHANG T, ZHANG W, TAKEUCHI A. Bulk Nd−Fe−Al amorphous alloys with hard magnetic properties [J]. Materials Transaction JIM, 1996, 37: 99−108.

熔体过热度对 $Nd_9Fe_{85-x}Ti_4C_2B_x$ (x=10, 12) 磁性合金过冷度和非晶形成的影响

杨梦琳，潘 晶，刘新才，肖晓燕，詹玉勇

宁波大学 材料科学与化学工程学院，宁波 315211

摘 要：采用差热分析及凝固组织研究 $Nd_9Fe_{85-x}Ti_4C_2B_x$ (x=10, 12)合金熔体过热度对其过冷度以及凝固组织的影响。结果表明：$Nd_9Fe_{85-x}Ti_4C_2B_x$ (x=10, 12)合金的过冷度随熔体过热度的增大而显著增大，且每种合金均出现两个对应于平均过冷度急剧增大的临界过热度。两个平均过冷度转折点的存在与过热熔体中的结构转变有关，这最终导致凝固组织中非晶相体积分数的增加。

关键词：磁性合金；熔体过热；过冷度；结构转变；非晶形成能力

(Edited by Wei-ping CHEN)